

Article

Low Temperature Deposition of TiO₂ Thin Films through Atmospheric Pressure Plasma Jet Processing

Suresh Gosavi^{1,2}, Rena Tabei³, Nitish Roy², Sanjay S. Latthe⁴, Yuvaraj M. Hunge², Norihiro Suzuki^{2,5}, Takeshi Kondo^{2,3,5}, Makoto Yuasa^{2,3,5}, Katsuya Teshima^{5,6}, Akira Fujishima² and Chiaki Terashima^{2,5,6,*}

- ¹ Center for Advance Studies in Material Science and Solid State Physics, Department of Physics, Savitribai PhulePune University, (Formerly University of Pune), Pune 411007, India; swg@physics.unipune.ac.in
- ² Photocatalysis International Research Center, Research Institute for Science and Technology, Tokyo University of Science, 2641 Yamazaki, Noda, Chiba 278-8510, Japan; nitu.iitg@gmail.com (N.R.); yuvihunge@gmail.com (Y.M.H.); suzuki.norihiro@rs.tus.ac.jp (N.S.); t-kondo@rs.tus.ac.jp (T.K.); yuasa@rs.tus.ac.jp (M.Y.); fujishima_akira@admin.tus.ac.jp (A.F.)
- ³ Faculty of Science and Technology, Tokyo University of Science, 2641 Yamazaki, Noda, Chiba 278-8510, Japan; 7216646@ed.tus.ac.jp
- ⁴ Raje Ramrao Mahavidyalaya, Jath 416404, India; latthes@gmail.com
- ⁵ Research Center for Space Colony, Tokyo University of Science, 2641 Yamazaki, Noda, Chiba 278-8510, Japan; teshima@shinshu-u.ac.jp
- ⁶ Research Initiative for Supra-Materials, Shinshu University, Nagano 380-8553, Japan
- * Correspondence: terashima@rs.tus.ac.jp

Abstract: Titanium dioxide (TiO₂) has been widely used as a catalyst material in different applications such as photocatalysis, solar cells, supercapacitor, and hydrogen production, due to its better chemical stability, high redox potential, wide band gap, and eco-friendly nature. In this work TiO₂ thin films have been deposited onto both glass and silicon substrates by the atmospheric pressure plasma jet (APPJ) technique. The structure and morphological properties of TiO₂ thin films are studied using different characterization techniques like X-ray diffraction (XRD), X-ray photoelectron spectroscopy (XPS), Raman spectroscopy, and field emission scanning electron microscopy. XRD study reveals the bronze-phase of TiO₂. The XPS study shows the presence of Ti, O, C, and N elements. The FE-SEM study shows the substrate surface is well covered with a nearly round shaped grain of different size. The optical study shows that all the deposited TiO₂ thin films exhibit strong absorption in the ultraviolet region. The oleic acid photocatalytic decomposition study demonstrates that the water contact angle decreased from 80.22 to 27.20° under ultraviolet illumination using a TiO₂ photocatalyst.

Keywords: atmospheric pressure plasma jet technique; TiO₂ thin films; photocatalytic; wettability



Citation: Gosavi, S.; Tabei, R.; Roy, N.; Latthe, S.S.; Hunge, Y.M.; Suzuki, N.; Kondo, T.; Yuasa, M.; Teshima, K.; Fujishima, A.; et al. Low Temperature Deposition of TiO₂ Thin Films through Atmospheric Pressure Plasma Jet Processing. *Catalysts* **2021**, *11*, 91. <https://doi.org/10.3390/catal11010091>

Received: 13 December 2020

Accepted: 8 January 2021

Published: 11 January 2021

Publisher's Note: MDPI stays neutral with regard to jurisdictional claims in published maps and institutional affiliations.



Copyright: © 2021 by the authors. Licensee MDPI, Basel, Switzerland. This article is an open access article distributed under the terms and conditions of the Creative Commons Attribution (CC BY) license (<https://creativecommons.org/licenses/by/4.0/>).

1. Introduction

TiO₂ is one of the most studied semiconductor oxide materials due to its vast applications, which include photocatalytic dye degradation, water splitting, self-cleaning agent, dye sensitized solar cells, photocatalytic hydrogen production, etc. Low cost synthesis, biocompatibility and inertness under ambient conditions are additional factors that make it one of the most studied materials [1,2]. Apart from these, it absorbs ultra violet (UV) light significantly so it is usable in cosmetics, such as sunscreen lotion. The UV light absorptions relate to its electronic transition from valence band (VB) to conduction band (CB). VB of TiO₂ is quite oxidative and hence its holes act as strong oxidant under UV light irradiation. Such band-to-band transition of TiO₂ by absorbing UV light and strong oxidant nature of the VB holes are the reasons behind the above-mentioned applications [3,4].

The cost of good quality coating depends on the processing parameters. The low pressure and temperature plasma technique is costly as well as inept due to the expensive vacuum system requirement and, in addition, utilization of different kinds and sizes of

substrates during the deposition process are limited [5]. Researchers have adopted different methods such as sol-gel, chemical vapor deposition, sputtering, pulsed laser deposition, electrodeposition and the spray pyrolysis method for deposition of the TiO₂ thin films. However, low temperature and atmospheric pressure plasma (APP) processing is a cost effective and versatile coating technique, which is tremendously attracting the interest of many research groups. However, it needs post heat treatment to achieve crystalline thin films. Recently, the atmospheric pressure plasma jet (APPJ) technique became more popular to obtain crystalline thin films in a single step without post-annealing. A plasma is generated by applying energy to a gas in order to rearrange the electronic structure of the atoms and molecules and to generate the excited species and ions. The generated energy can be thermal or carried by either an electric current or electromagnetic radiations. The APPJ is a small RF plasma torch that works at low power. It consists of two concentric electrodes through which a mixture of helium, oxygen, and other gases flow. By applying RF power between 1 to 100 MHz to the inner electrode at a voltage between 100–250 V, the gas discharge is ignited. The ionized gas from the plasma jet exits through a nozzle, where it is directed onto a substrate a few millimeters downstream. The low injected power enables the torch to produce a stable discharge and avoids the arc transition. The APP and APPJ techniques are thoroughly discussed in the recent review article [5–7].

In recent times, Dong and co-researchers achieved adherent, optically transparent and fine electrically conductive TiN_x/TiO₂ hybrid films on polycarbonate and silicon substrates using the APP technique [8]. The plasma processing conditions, i.e., power and gas compositions, were precisely varied to achieve the hybrid thin films with 83% transmittance in the visible region, almost 8.5 J/m² of film adhesion energy towards the polycarbonate and electrical resistivity of $\sim 8.5 \times 10^1$ ohm cm before annealing. Post annealing and submission of H₂ gas into the primary plasma have successfully reduced the electrical resistivity of the hybrid film to $\sim 6.1 \times 10^{-1}$ ohm cm. Chou et al. have used the APP method to deposit anatase TiO₂ nano-dendrites (TNDs) films on FTO substrates for dye sensitized solar cell (DSSC) applications [9]. Due to high specific surface area of the ordered TNDs films, a photo-conversion efficiency of 12.08 % was achieved under simulated AM 1.5 solar light irradiation. Gazal et al. have studied the growth of TiO₂ films on silicon substrates using the APP-ECVD-microwave torch method [10]. A TiO₂ film got deposited in circular shape as a consequence of plasma jet geometry, which affects the film thickness as well as crystallinity from the center to periphery. The crystalline anatase phase TiO₂ with precise columnar growth was observed at the center, whereas crystallinity eventually vanished at the periphery with cauliflower-like amorphous structure. The improved photocatalytic properties of TiO₂ can be observed by synthesizing the TiO₂ material with both anatase and rutile phases, which assist in diminishing the possibility of electron-hole recombination [11]. Recently, Wang et al. synthesized the mixed phase anatase-rutile TiO₂ nanopowders using the APPJ technique [12]. Chang et al. synthesized dye-sensitized solar cells (DSSCs) with TiO₂ photoanodes sintered by N₂ and air atmospheric pressure plasma jets (APPJs) with/without air-quenching [13].

In the present research work, the APPJ technique was used to deposit TiO₂ thin films onto the glass and silicon substrates. This technique enables thin film deposition on large or any type of substrate without the need for vacuum or inert deposition environments. Also, this technique is useful for obtaining crystalline thin films in a single step without post-annealing or post-deposition treatments. Helium gas and argon (Ar) gas are used as the carrier gas and H₂O vapor is also introduced. The fixed flow rate was maintained for Helium gas and H₂O vapor 5.0 and 20 mL/min, respectively. By varying the Argon gas flow rate 50 and 300 mL/min for the depositions TiO₂ thin films. The deposited TiO₂ thin films are characterized using the different characterization tools like, XRD, XPS, Raman Spectroscopy, FE-SEM, contact angle, and UV-Vis spectra in diffused reflection mode.

2. Results and Discussion

An X-ray diffraction study was used to confirm the crystal structure of the prepared TiO₂ thin films. Figure 1 shows the XRD patterns of TiO₂ thin films deposited at fixed flow rate of He = 5 L/min as a carrier gas, and Ar flow rate of 50 and 300 mL/min and recorded by varying the diffraction angle (2θ) from 20° to 80°.

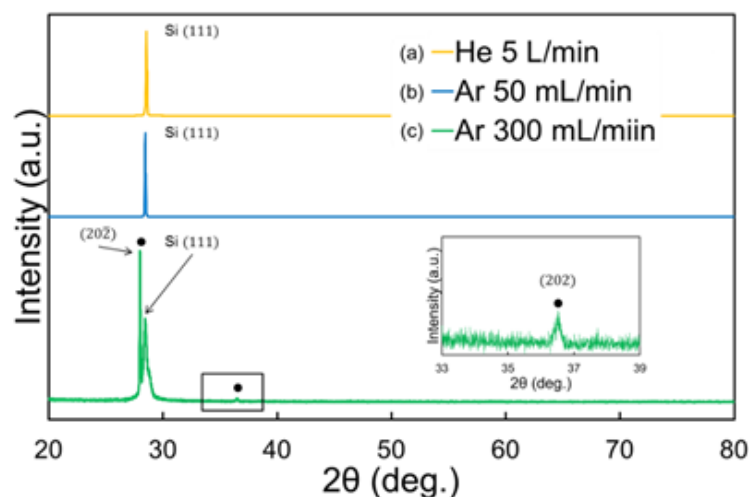


Figure 1. X-ray diffraction patterns of TiO₂ thin films deposited using the atmospheric pressure plasma jet technique with H₂O vapor at fixed flow rate (500 mL/min) of titanium ethoxide precursor and (a) He = 5 L/min (b) He = 5L/min + Ar = 50mL/min and (c) He = 5L/min + Ar = 300 mL/min.

All XRD patterns shows the peak (111) arises from the Si substrate. For TiO₂ samples deposited at He = 5 L/min and 50 mL/min no diffraction peaks TiO₂ were detected, which suggests an amorphous nature or that the nanocrystals are smaller than the detection limit of the XRD set-up [14,15]. For TiO₂ sample deposited at Ar = 300 mL/min shows the diffraction peak at $2\theta = 36.14^\circ$, corresponding to the (202) plane, which is in well agreement with JCPDS card no. 46-1237 and confirms the bronze-phase of TiO₂ [16].

Symmetry and modes of vibration present in the TiO₂ structure is studied with the help of Raman spectroscopy. Figure 2A,B shows the Raman spectra of TiO₂ thin films with and without H₂O vapor flow.

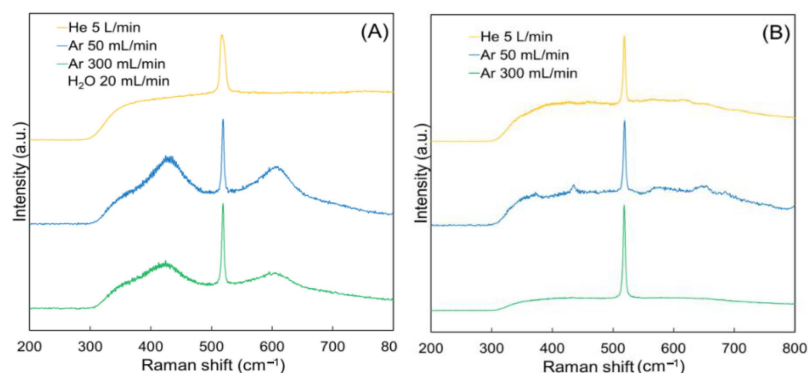


Figure 2. (A) Raman spectra of TiO₂ thin films with H₂O flow rate 20 mL/min, (B) without H₂O flow rate.

All TiO₂ spectra show the strong peak at 520 cm⁻¹, which is associated with the Si substrate [17]. The Raman peak found at 418 cm⁻¹ corresponds to the A_g vibrational mode found in the sample prepared using H₂O vapor and Ar flow rate of 50 and 300 mL/min (Figure 2A) [18]. While, in the case of He gas, the Raman peak at 418 cm⁻¹ is not observed, indicating the amorphous nature of the TiO₂. The degree of crystallinity is higher at a

low gas flow rate of Ar (50 mL/min). Figure 2B shows without H₂O vapor all samples exhibit the amorphous nature of TiO₂, while the sample prepared at gas flow rate of Ar (50 mL/min) shows a peak at 418 cm⁻¹.

For crystallized films (i.e., synthesized with H₂O vapor), an XPS study was used to analyze chemical composition and surface state of the elements present in the TiO₂ sample. Figure 3A displays the survey scan spectrum of the TiO₂ sample prepared at a gas flow rate of He = 5L/min + Ar = 300 mL/min. It shows the signals of C1s, O1s, Ti2p, N1s elements and Si substrate peak present in TiO₂. No other elements or impurity peaks were found in the prepared sample. Figure 3B shows the Ti 2p spectrum. Due to the spin orbit coupling the Ti 2p spectrum split into two stronger and two weaker peaks at binding energy 464.4, 458.5 eV and 462 and 456.5 eV, respectively.

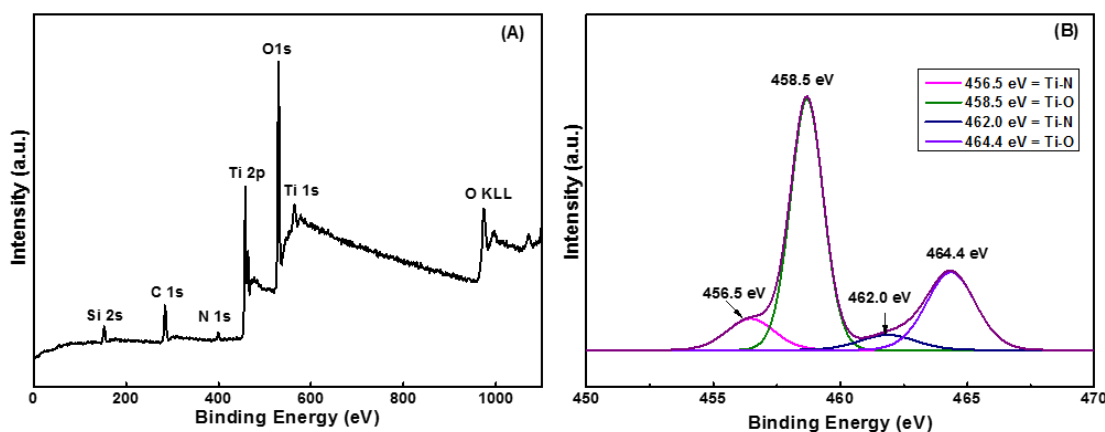


Figure 3. (A) Survey scan spectrum and (B) Ti2p spectrum of TiO₂ thin films deposited using Atmospheric Pressure Plasma Jet with H₂O vapor at fixed flow rate (500 mL/min) of Titanium ethoxide precursor and He = 5L/min + Ar = 300 mL/min.

The peaks at binding energy 464.4 and 458.5 eV associated with the Ti2p_{1/2} and Ti2p_{3/2} components, respectively [19]. The binding energy difference between the two peaks is 5.9 eV, which is in good agreement with reported values attributed to Ti⁴⁺ confirming the formation of the TiO₂ compound [20]. The peaks were at binding energy 458.5 and 462.0 eV associated with Ti-N bonding. The observed higher O1s concentration and N1s species is considered to be due to the atmospheric processes. Elemental analysis using XPS for a synthesized TiO₂ thin film with its atomic percentage is given in Table 1. Since the synthesis is carried out in an atmosphere, as expected, the Nitrogen functionality with small atomic percentage is observed. The atomic percentage for Ti2p varies from 37.18% to 43.91% and for O1s it is 38.10%, to 42.41%, respectively. Table 2 shows the ratio of Ti-N and Ti-O at 5 mm distance between substrate and plasma plume.

Table 1. Difference in atomic percentage of Ti, O, C and N elements at different deposition conditions. Distance between the plasma jet and a substrate are shown in the parenthesis.

	Mass (%)			
	Ti (2p)	O (1s)	C (1s)	N (1s)
Ar 50 mL/min (5 mm)	37.18	42.41	17.63	2.78
Ar 50 mL/min (1 mm)	39.02	44.47	14.58	1.93
Ar 300 mL/min (5 mm)	36.72	43.29	17.65	2.34
Ar 300 mL/min (1 mm)	43.91	38.10	16.58	1.40

Table 2. Ratio of Ti-N and Ti-O at 5 mm distance between substrate and plasma plume.

	Mass (%)			
	Ti-N (456 eV)	Ti-O (459 eV)	Ti-N (462 eV)	Ti-O (464 eV)
Ar 50 mL/min (5 mm)	22.97	45.92	16.34	14.77
Ar 300 mL/min (5 mm)	10.29	57.30	5.88	26.53

The film thickness was measured using a cross section of the films for different flow rates of Ar, He gases and water vapor. Figure 4A–C shows the cross section view of TiO₂ thin films using SEM. For the He and H₂O flow rate (He = 5L/min + H₂O = 20 mL/min) TiO₂ film thickness was observed to be 4 μm. While in the case of Ar, the gas flow rate increased from 50 to 300 mL/min, and it is observed that film thickness increased from 2 to 3 μm. This increase in film thickness attributed to the Ar gas flow can enhance the energetic ion bombardment, which promotes the mobility of atoms, and also, when there is a further increase in Ar gas flow, the ion density becomes large enough for crystal growth; hence, the grain size [21].

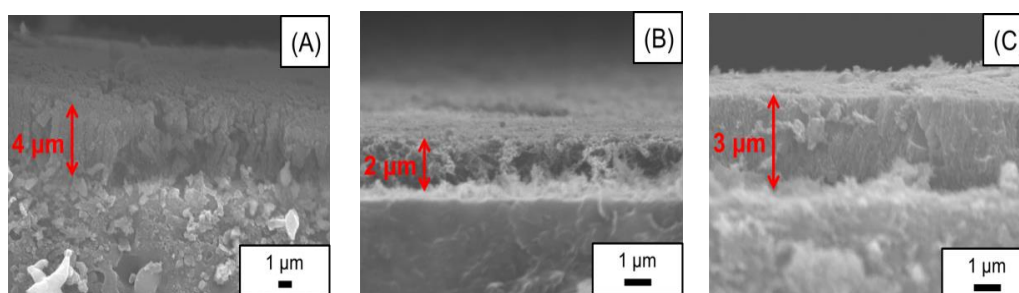


Figure 4. Cross sectional view of TiO₂ thin films deposited at (A) He = 5L/min + H₂O = 20 mL/min (B) He = 5L/min + Ar = 50 mL/min + H₂O = 20 mL/min and (C) He = 5L/min + Ar = 300 mL/min + H₂O = 20 mL/min; using atmospheric pressure plasma jet.

Figure 5A–F shows the SEM images of TiO₂ thin films prepared at different deposition conditions. For the TiO₂ sample (Figure 5A) prepared at He = 5L/min without the water vapor condition, clubbed shape grains are observed, then fairly spherical shaped after water vapor was introduced (Figure 5B) and particle size reduced. Reduction of particle size was observed after the addition of water vapor in all cases (Figure 5D,F).

In the case (Figure 5 C) of Ar gas of 30 mL/min and without water vapor composition, TiO₂ nanoparticles are agglomerated and with water vapor particles, the size reduced. While for the Ar gas of flow rate 300 mL/min and without water vapor, nearly round shaped TiO₂ grains are observed (Figure 5E) and after introducing water vapor, grain size is reduced (Figure 5F). For different gases (He and Ar), morphology is different. Also, for the same gas (Ar) but different flow rate (50 and 300 mL/min), different morphology is observed, which suggests that gas flow rate and mixture of different gases affects the morphology [22,23].

Figure 6 shows the UV-vis spectra in diffused reflection mode for TiO₂ thin films deposited at fixed flow rate of He = 5 L/min as a carrier gas, and Ar flow rate of 50 and 300 mL/min. All the deposited TiO₂ thin films exhibit the strong absorbance in the UV region whereas high transmittance in the visible range. The band gap of the deposited TiO₂ thin films varies from 3.87 to 4.07 eV. The band edge is shifted towards the higher energy side indicating a red shift. In the case of Ar, the gas flow rate increased and the reflectance decreased, which suggests that the flow rate of the gas affects the optical properties of TiO₂ thin films [24].

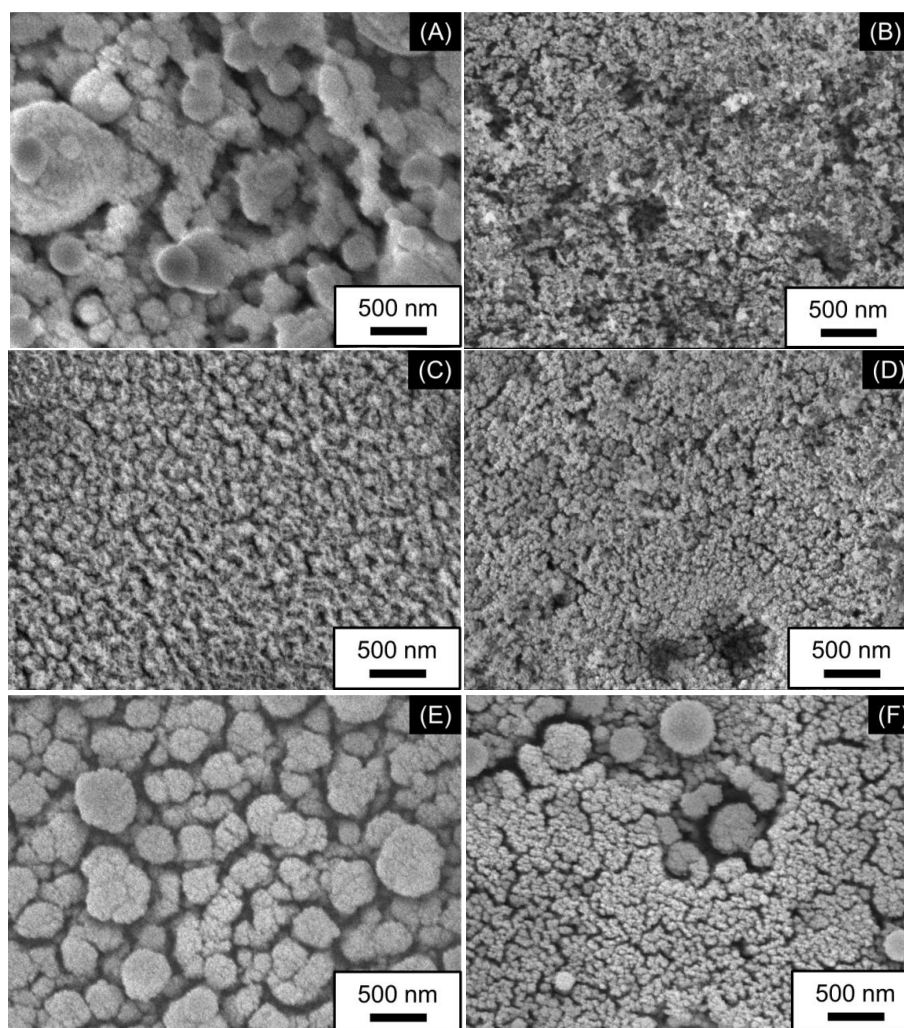


Figure 5. SEM images of TiO₂ thin films (A) without and (B) with water vapor for He = 5 L/min, (C) without and (D) with water vapor for He = 5 L/min + Ar = 50 mL/min, and (E) without and (F) with water vapor for He = 5 L/min + Ar = 300 mL/min.

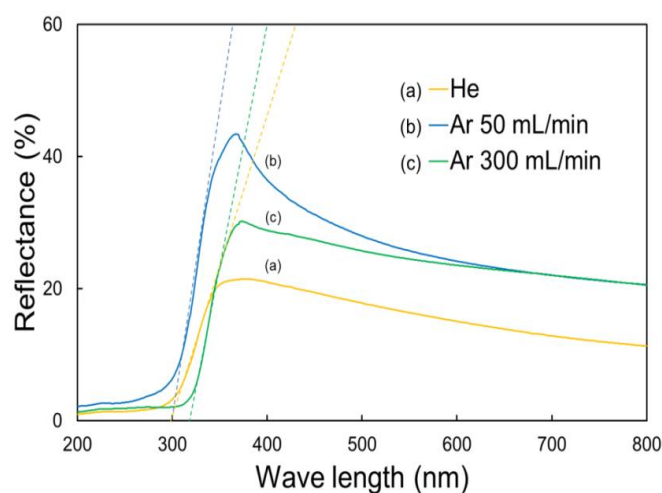


Figure 6. UV-vis diffused reflectance spectra for TiO₂ thin films deposited using atmospheric pressure plasma jet at fixed flow rate (500 mL/min) of titanium ethoxide precursor and (a) He = 5L/min (b) He = 5L/min + Ar = 50mL/min and (c) He = 5L/min + Ar = 300 mL/min.

Figure 7 presents the photocatalytic decomposition study of Oleic acid using bare glass and TiO₂ thin films. The photocatalytic activity of the bare glass and TiO₂ thin films (He/Ar: 3L/min / 300 mL/min and water vapor) prepared by the APPJ technique was tested for the photocatalytic decomposition of oleic acid under UV light illumination. For glass substrate coated with oleic acid, a nearly constant (about 43°) water contact angle was observed up to 25 h under UV light illumination. No major changes are observed in the water contact angle after 25 h illumination, which proves that no photocatalytic decomposition of oleic acid takes place on the surface of glass substrate under ultraviolet light illumination in the absence of TiO₂ coating.

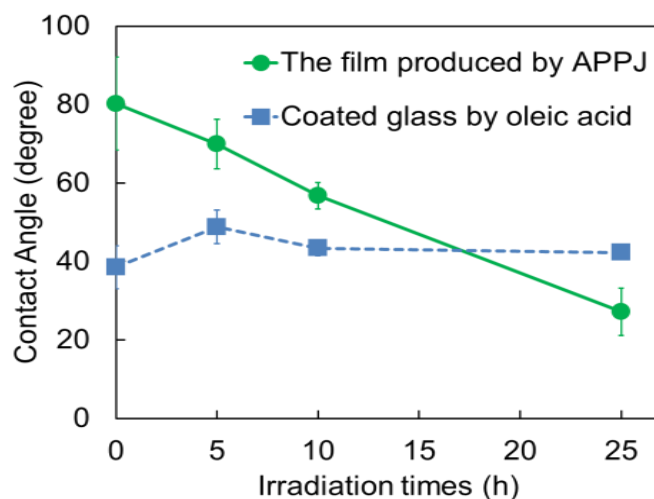


Figure 7. Photocatalytic decomposition of oleic acid using bare glass and TiO₂ thin films.

Similar experiments were performed using TiO₂ thin films. Before UV irradiation, the water contact angle was 80.22°, which shows that oleic acid was successfully coated on the TiO₂ surface. The oleic acid treated TiO₂ photocatalyst was exposed to UV light and, as a result, the water contact angle decreased slowly from 80.22° to 27.2° during 25 h of irradiation time. The decrease in water contact angle after UV irradiation confirms the photocatalytic decomposition of oleic acid using the TiO₂ photocatalyst. These results suggest that both light and catalyst is required for the effective photocatalytic decomposition of organic compounds like oleic acid [25,26].

3. Experimental

3.1. Materials

Titanium ethoxide (Ti₄(OCH₂CH₃)₁₆) was purchased from Sigma-Aldrich. Oleic acid (C₁₈H₃₄O₂), and n-heptane (C₇H₁₆) were purchased from the Fujifilm Wako Pure Chemical Corporation (Osaka, Japan). These chemicals were used as obtained.

3.2. Synthesis of TiO₂ Thin Film

The APPJ experimental set up was developed and presented through the schematic diagram in Figure 8. The jet was made up of a Pyrex glass tube with a 4 mm diameter, which is capacitively coupled to the pulse generator by using copper electrode (research grade (99.99%)). Helium gas and argon (Ar) gas were used as carrier gas, whereas Titanium ethoxide was used as a precursor source, which was kept at a temperature of 125 °C. H₂O vapor was also introduced. The plasma was sustained using an AC pulsed power supply at 15 KHz frequency having 1 μs pulsed rate by keeping discharge voltage constant at 4 kV corresponding to 160 Watts. Optimization of atmospheric pressure plasma deposition parameters for TiO₂ thin film were carried out with fixed flow rate of helium gas = 5.0 L/min, and plasma was sustained in the jet, which shows violet plasma. By keeping the precursor (titanium ethoxide MW 228.11 gm/mol) flow rate constant = 500 mL/min and varying the

argon gas flow rate from 50 to 300 mL/min, depositions of TiO₂ were carried out with and without H₂O vapor. The flow rate for H₂O vapor was maintained at 20 mL/min. The deposition time was kept constant at 5 min for all the cases. The substrate to plasma jet distance was basically kept constant at 5 mm, throughout the experiments where the plume was uniformly distributed with high plasma density.

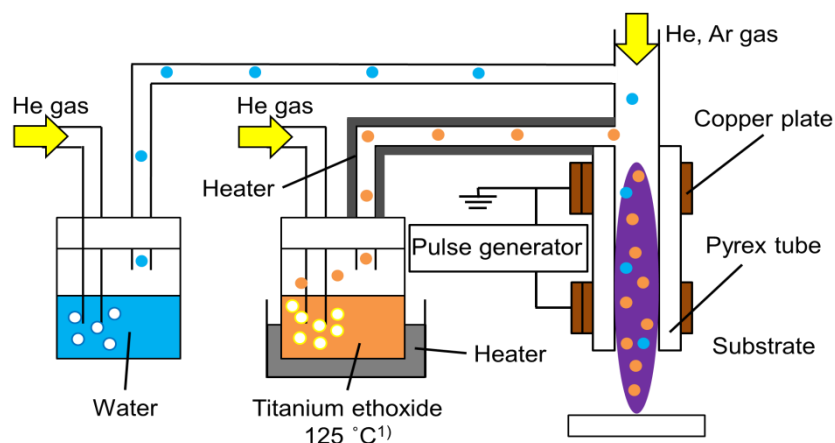


Figure 8. Schematic diagram of experimental setup used for the synthesis of TiO₂ thin films using atmospheric pressure plasma jet.

3.3. Photocatalytic Activity Test

The photocatalytic activity test of APPJ synthesized TiO₂ thin films and bare glass were studied by performing photocatalytic decomposition of oleic acid. In order to remove the residual organic components present on the surface of TiO₂ thin film, it was pre-treated before the photocatalytic experiment using UV light with a wavelength of 365 nm at 2.0 mW cm⁻² for a single day. After one day of UV illumination, the TiO₂ thin film was immersed in 0.5 vol% oleic acid solution diluted with n-heptane, and then withdrawn using a dip-coater at 10 mm s⁻¹. To dry the oleic acid layer, samples were heated at 70 °C for 15 min with a hot plate. The samples were illuminated with 365 nm UV light at 1.0 mW cm⁻² to induce photocatalytic decomposition of oleic acid. During the test, samples were taken at different time intervals and the water-contact angle measurement was carried out using a contact angle meter (DM-501, Kyowa Interface Science Co., Ltd.) [26].

3.4. Characterization Technique Details

Structural, morphological, and optical characterization, of the deposited TiO₂ thin film was carried out by using XRD, XPS, Raman, FE-SEM and UV-Vis techniques. X-ray diffraction (XRD) analyses were performed on a Bruker D8 Discover diffractometer with a CuK_α radiation source in detector mode at 1.0 degree grazing incidence. XPS analysis of the film was carried out using an AXIS Nova X-ray photoelectron spectrometer. The system was equipped with AlK_α radiation source (1486.6 eV), which was operated at 150 W, having a spectral resolution of 0.1 eV. The system was operated at the base pressure of 1.0 × 10⁻⁹ Pa. The binding energy (BE) values are charge-corrected to C 1s = 284.6 eV as an internal standard, and the pass energy of 40 eV was used. Raman spectra were collected on a NRS-510, JASCO Raman microscope, using an excitation wavelength of 532 nm. Morphologies of as-deposited thin film samples were observed using field emission scanning electron microscopy (FE-SEM, JSM 7600F), operated at 20 kV, with 1.0 nm resolution. The film thickness was measured by using an SEM cross section, using a lapping technique. UV-Vis spectra in diffused reflection mode were recorded using a JASCO V-670 spectrophotometer at 2 nm resolution within the range 200–800 nm.

4. Conclusions

The TiO₂ thin films can successfully be deposited onto glass and Si substrates using the APPJ technique. The XRD, Raman and XPS study confirms the formation of TiO₂ by the APPJ technique. This technique is useful for thin film deposition of any type of substrate without the need for vacuum or inert deposition environments. Also, it is useful to obtain crystalline thin films in a single step without post-annealing or post-deposition treatments. Also, the effect of gases like He, Ar, water vapor and gas flow rate on the structural, morphological, optical properties of TiO₂ thin films was studied. Different gas composition and flow rate affect the structural, morphology and optical properties. From the SEM study, it is observed that particle size of TiO₂ decreased after introducing water vapor during synthesis. Also, the SEM cross sectional study shows that an increase in Ar gas flow rate increased film thickness. The oleic acid photocatalytic decomposition experiment shows that the water contact angle decreased, which confirms the photocatalytic decomposition of oleic acid under ultraviolet light illumination.

Author Contributions: S.G.: Data curation, Formal analysis, Investigation, Writing-original draft. R.T.: Investigation, Experimental, Analysis, Data curation. N.R.: Formal analysis, Investigation. S.S.L.: Formal analysis, Investigation. Y.M.H.: Writing-original draft. N.S.: Investigation, Methodology. T.K.: Formal analysis, Investigation. M.Y.: Data curation, Formal analysis, Investigation. K.T.: Methodology. A.F.: Conceptualization, Project administration, Supervision. C.T.: Project administration, Supervision, Conceptualization, Methodology. All authors have read and agreed to the published version of the manuscript.

Funding: This study was partly supported by MEXT Promotion of Distinctive Joint Research Center Program Grant Number JPMXP0618217662.

Institutional Review Board Statement: Not applicable.

Informed Consent Statement: Not applicable.

Data Availability Statement: Data is contained within the article.

Conflicts of Interest: The authors declare no conflict of interest.

References

1. Linsebigler, A.L.; Lu, G.; Yates, J.T., Jr. Photocatalysis on TiO₂ Surfaces: Principles, Mechanisms, and Selected Results. *Chem. Rev.* **1995**, *95*, 735–758. [[CrossRef](#)]
2. Fan, Q.; McQuillin, B.; Ray, A.K.; Turner, M.L.; Seddon, A.B. High density, non-porous anatase titania thin films for device applications. *J. Phys. D Appl. Phys.* **2000**, *3*, 2683–2686. [[CrossRef](#)]
3. Hashimoto, K.; Irie, H.; Fujishima, A. TiO₂ photocatalysis: A historical overview and future prospects. *Jpn. J. Appl. Phys.* **2005**, *44*, 8269. [[CrossRef](#)]
4. Hunge, Y.M.; Yadav, A.A.; Khan, S.; Takagi, K.; Suzuki, N.; Teshima, K.; Terashima, C.; Fujishima, A. Photocatalytic degradation of bisphenol A using titanium dioxide@nanodiamond composites under UV light illumination. *J. Colloid Interface Sci.* **2021**, *582*, 1058–1066. [[CrossRef](#)] [[PubMed](#)]
5. Schutze, A.; Jeong, J.Y.; Babayan, S.E.; Park, J.; Selwyn, G.S.; Hicks, R.F. The atmospheric-pressure plasma jet: A review and comparison to other plasma sources. *IEEE Trans. Plasma Sci.* **1998**, *26*, 1685–1693. [[CrossRef](#)]
6. Mariotti, D.; Belmonte, T.; Benedikt, J.; Velusamy, T.; Jain, G.; Švrček, V. Low-Temperature Atmospheric Pressure Plasma Processes for “Green” Third Generation Photovoltaics. *Plasma Process. Polym.* **2016**, *13*, 70–90. [[CrossRef](#)]
7. Tendero, C.; Tixier, C.; Tristant, P.; Desmaison, J.; Leprince, P. Atmospheric pressure plasmas: A review. *Spectrochim. Acta B* **2006**, *61*, 2–30. [[CrossRef](#)]
8. Dong, S.; Watanabe, M.; Dauskardt, R.H. Conductive Transparent TiN_x/TiO₂ Hybrid Films Deposited on Plastics in Air Using Atmospheric Plasma Processing. *Adv. Funct. Mater.* **2014**, *24*, 3075–3081. [[CrossRef](#)]
9. Chou, W.C.; Liu, W.J. Study of dye sensitized solar cell application of TiO₂ films by atmospheric pressure plasma deposition method. In Proceedings of the International Conference on Electronics Packaging (ICEP), Sapporo, Japan, 20–22 April 2016.
10. Gazal, Y.; Dublanche-Tixier, C.; Chazelas, C.; Colas, M.; Carles, P.; Tristant, P. Multi-structural TiO₂ film synthesized by an atmospheric pressure plasma-enhanced chemical vapor deposition microwave torch. *Thin Solid Films* **2016**, *600*, 43–52. [[CrossRef](#)]
11. Liu, G.; Yan, X.; Chen, Z.; Wang, X.; Wang, L.; Lu, G.Q.; Cheng, H.M. Synthesis of rutile-anatase core-shell structured TiO₂ for photocatalysis. *J. Mater. Chem.* **2009**, *19*, 6590–6596. [[CrossRef](#)]

12. Wang, Y.; Yuan, Q.; Yin, G.; Zhang, Y.; Zhang, Y.; Li, Y.; Li, J.; Wang, T.; Ma, S. Synthesis of Mixed-Phase TiO₂ Nanopowders Using Atmospheric Pressure Plasma Jet Driven by Dual-Frequency Power Sources. *Plasma Chem. Plasma Process.* **2016**, *36*, 1471–1484. [[CrossRef](#)]
13. Chang, H.; Hsu, C.M.; Kao, P.K.; Yang, Y.J.; Hsu, C.C.; Cheng, I.C.; Chen, J.Z. Dye-sensitized solar cells with nanoporous TiO₂ photoanodes sintered by N₂ and air atmospheric pressure plasma jets with/without air-quenching. *J. Power Source* **2014**, *251*, 215–221. [[CrossRef](#)]
14. Suzuki, N.; Terashima, C.; Nakata, K.; Katsumata, K.; Fujishima, A. Synthesis of a mesoporous titania thin film with a pseudo-single-crystal framework by liquid-phase epitaxial growth, and enhancement of photocatalytic activity. *RSC Adv.* **2020**, *10*, 40658–40662. [[CrossRef](#)]
15. Yasuda, H.; Hirotsu, T. Critical Evaluation of Conditions of Plasma Polymerization. *J. Polym. Sci. Polym. Chem. Ed.* **1978**, *16*, 743–759. [[CrossRef](#)]
16. Fakhouri, H.; Salem, D.B.; Carton, O.; Pulpytel, J.; Khonsari, F.A. Highly efficient photocatalytic TiO₂ coatings deposited by open air atmospheric pressure plasma jet with aerosolized TTIP precursor. *J. Phys. D Appl. Phys.* **2014**, *47*, 265301. [[CrossRef](#)]
17. Zhou, Y.; Zhu, Q.; Tian, J.; Jiang, F. TiO₂ Nanobelt@Co9S8 Composites as Promising Anode Materials for Lithium and Sodium Ion Batteries. *Nanomaterials* **2017**, *7*, 252. [[CrossRef](#)]
18. Borowicz, P.; Latek, M.; Rzedkiewicz, W.; Łaszcz, A.; Czerwinski, A.; Ratajczak, J. Deep-ultraviolet Raman investigation of silicon oxide: Thin film on silicon substrate versus bulk material. *Adv. Nat. Sci. Nanosci. Nanotechnol.* **2012**, *3*, 045003. [[CrossRef](#)]
19. Jokisaari, J.R.; Bayerl, D.; Zhang, K.; Xie, L.; Nie, Y.; Schlom, D.G.; Kioupakis, E.; Graham, G.W.; Pan, X. Polarization-Dependent Raman Spectroscopy of Epitaxial TiO₂(B) Thin Films. *Chem. Mater.* **2015**, *27*, 7896–7902. [[CrossRef](#)]
20. Hunge, Y.M.; Yadav, A.A.; Dhodamani, A.G.; Suzuki, N.; Terashima, C.; Fujishima, A.; Mathe, V.L. Enhanced photocatalytic performance of ultrasound treated GO/TiO₂ composite for photocatalytic degradation of salicylic acid under sunlight illumination. *Ultrason. Sonochem.* **2020**, *61*, 104849. [[CrossRef](#)]
21. Hernandez-Rodriguez, E.; Marquez-Herrera, A.; Zaleta-Alejandre, E.; Melendez-Lira, M.; Cruz, W.D.; Zapata-Torres, M. Effect of electrode type in the resistive switching behavior of TiO₂ thin films. *J. Phys. D Appl. Phys.* **2013**, *46*, 045103. [[CrossRef](#)]
22. Vijaya, G.; Singh, M.M.; Krupashankara, M.S.; Kulkarni, R.S. Effect of Argon Gas Flow Rate on the Optical and Mechanical Properties of Sputtered Tungsten Thin Film Coatings. *IOP Conf. Ser. Mater. Sci. Eng.* **2016**, *149*, 012075. [[CrossRef](#)]
23. Zurek, J.; Michalik, M.; Schmitz, F.; Kern, T.U.; Singheiser, L.; Quadackers, W.J. The Effect of Water-Vapor Content and Gas Flow Rate on the Oxidation Mechanism of a 10% Cr-Ferritic Steel in Ar-H₂O Mixtures. *Oxid. Met.* **2005**, *63*, 401–422. [[CrossRef](#)]
24. Rebrov, A.K.; Emelyanov, A.A.; Plotnikov, M.Y.; Timoshenko, N.I.; Terekhov, V.V.; Yudin, I.B. Effect of the gas mixture flow rate on the process of diamond synthesis from a high-velocity microwave plasma. *J. Appl. Mech. Tech. Phys.* **2020**, *61*, 819–827. [[CrossRef](#)]
25. Jena, S.; Tokas, R.B.; Misal, J.S.; Rao, K.D.; Udupa, D.V.; Thakur, S.; Sahoo, N.K. Effect of O₂/Ar gas flow ratio on the optical properties and mechanical stress of sputtered HfO₂ thin films. *Thin Solid Films* **2015**, *592*, 135–142. [[CrossRef](#)]
26. Adachi, T.; Latthe, S.S.; Gosavi, S.W.; Roy, N.; Suzuki, N.; Ikari, H.; Kato, K.; Katsumata, K.; Nakata, K.; Furudate, M.; et al. Photocatalytic, superhydrophilic, self-cleaning TiO₂ coating on cheap, light-weight, flexible polycarbonate substrates. *Appl. Surf. Sci.* **2018**, *458*, 917–923. [[CrossRef](#)]